Received 2 February 2024; revised 9 March 2024; accepted 11 March 2024. Date of publication 18 March 2024; date of current version 27 May 2024.

Digital Object Identifier 10.1109/OJAP.2024.3377695

Low-Profile CO-CSRR and EBG Loaded Tri-Quarter Circular Patch EWB MIMO Antenna With Multiple Notch Bands

HEMALATHA T, (Member, IEEE), AND BAPPADITTYA ROY (Senior Member, IEEE)

School of Electronics Engineering, VIT-AP University, Amaravati 522237, India

CORRESPONDING AUTHOR: B. ROY (e-mail: bappadittya.roy@vitap.ac.in)

ABSTRACT A novel and miniaturized design featuring a Co-directional Complementary Split Ring Resonator (CO-CSRR) loaded Tri-Quarter Circular (TQC) Extremely Wideband (EWB) Multiple-Input Multiple-Output (MIMO) antenna has been developed and simulated. This proposed antenna demonstrates high isolation and exhibits multiple notch characteristics. The configuration consists of two TQC patches positioned adjacent to each other with a common partial ground plane (PGP), achieving an Extremely Wideband (EWB) capability of 85.8 GHz. Additionally, two elliptical CO-CSRRs are etched on the TQC elements to introduce dual-notch characteristics in the X-band and Ku-band. The integration of two Electromagnetic Band Gap (EBG) structures on either side of the microstrip feedline facilitates the creation of notch frequency ranges at Q-band downlink and V-band. To enhance isolation, a slotted meandering strip is extruded to the PGP. This design primarily focuses on achieving EWB with a compact size and reduced complexity. The overall physical volume of the proposed design is 2.74 $\lambda_o \times 4.83\ \lambda_o \times 0.25\ \lambda_o$, achieved a maximum $|S_{11}|$ of 30.82 dB at a frequency of 17.58 GHz. The antenna's performance has been thoroughly evaluated in terms of radiation pattern, isolation, Total Active Reflection Coefficient (TARC), Envelope Correlation Coefficient (ECC), Diversity Gain (DG), Gain, and Efficiency. Stable gain and Group Delay (GD) of less than 0.2 ns for the entire Extremely Wideband (EWB) range have been achieved, with lower gain observed at the notch bands.

INDEX TERMS Circular patch, EBG, extremely wideband, isolation, meandering slot, MIMO, notch.

I. INTRODUCTION

WIRELESS communication has witnessed significant advancements over the years, driven by technological innovations, evolving standards, and growing demand for faster and more reliable wireless connectivity. By using less power and enhanced bandwidth, MIMO technology reduces multipath fading and increases data transmission capacity when compared to single-antenna systems. In order to minimise mutual coupling and attain dependable performance, numerous antennas are arranged in an orthogonal or parallel design [1]. Wideband and high isolation features for a particular MIMO antenna is a challenging task. In [2], eight radiating elements accommodated in a precise imprint, each pair of radiating elements are placed in orthogonal configuration. An annular-reflector conjoined with the ground plane to enhance the isolation. Several methods to achieve super UWB characteristics include eye-shaped slotted circular patch [3], hybrid fractal [4], inverted U-shaped, C and Y-shaped slots at different positions and resonator lengths [5], loading parasitic stubs on the ground plane [6], [7]. Various scholarly works have highlighted diverse methodologies for achieving UWB, aiming to enhance frequency coverage. However, it is important to note that these approaches, while contributing to improved performance, may also added intricacies in the design process. In this research work, a simple three-fourth circular patch with partial ground plane is used to achieve the extremely wideband frequency coverage.

A 10-element MIMO antenna for LTE 42, 43 and 46 bands using a double T-elements was proposed in [8], no additional decoupling networks were introduced to reduce the mutual coupling and achieved the channel capacity of 41 bps/Hz at 20 dB Signal-to-Noise Ratio (SNR). In [9], the authors meticulously engineered a high-performance 18-element antenna on FR4 substrate for 4G and 5G

compatibility, achieving a bandwidth exceeding 900 MHz. They optimized impedance matching using a T-shaped feed line. Additionally, they implemented open-ended slots to minimize mutual coupling between adjacent antenna elements. A defected co-planar waveguide fed shovel antenna with super wideband MIMO [10] covered the operating frequency range from 4.1 to 60 GHz with a notch band of 6.8 to 7.8 GHz. Koch snowflake fractal in consolidation with a CSRR proposed in [11] realized a fractional bandwidth of 25.08%. Edge truncated rectangular patch engraved with circular slot and ground length variations provided optimum return loss [12], Mushroom and uniplanar EBG unit cells [13]. Circular ring shaped patch element placed in orthogonal configuration and also frequency selective surface employed to circular ring shaped MIMO for enhancement of directivity, also reduced the back lobe radiation [14], a straight solid strip at the top of a three-stage, dual-sided staircase with a Defected Ground Structure [15], step quarter-wave impedance transformer technique [16], loop-based split ring resonators [17] are different methods proposed by researchers for the enrichment of antenna performance. It is challenging to designate many frequency notches in compact UWB MIMO antennas because of the space constraints placed on the antenna.

UWB signals typically have large bandwidths, and the antennas need to be designed to cover this wide frequency range. This can lead to larger physical antenna sizes [18]. Increasing the amount of antennas in a MIMO array can enhance system performance, but it also increases the complexity of the overall system. Dense antenna element arrangements can cause radiation pattern distortion, which will adversely impact system capacity and diversity gain performance. The trade-off between size and complexity is one of the challenging issue, which involves a balance research to improve the compactness and minimize the complexity without compromising the antenna performance. Few researchers reduced the physical volume of the antenna and enhanced the system performance by introducing curved stub, split square ring shaped slot, inverted F-antenna [19] a fractional bandwidth of 12% is realized with 50% radiation efficiency, n-section tapered feedline [20], spade shaped patch with DGS [21], circular disc [22].

The literature places a significant emphasis on UWB MIMO systems, highlighting the importance of achieving high isolation and incorporating multiple notch bands. However, it is acknowledged that the presence of additional intricacies has contributed to heightened complexity, making implementation more challenging. The challenging issues like compactness, super UWB with enhanced isolation and notch characteristics are taken into account and developed a novel and miniaturized EWB MIMO with TQC radiating elements using High Frequency Structure Simulator (HFSS). Two slots and two EBG structures are etched to achieve the multiple band-notched characteristics. Meandering slot is etched on the PGP to enhance the isolation for the entire EWB. A parametric investigation is carried out to the proposed antenna for different ground widths different isolation techniques. The paper is categorize as follows: Section II narrate the design evolution and notch characteristics of the proposed antenna. Section III illustrates the simulation results and analysis of experimental results attained from the fabricated prototype, followed by conclusion in Section IV.

TABLE 1. Dimensions of the TQC EWB MIMO (in mm).

Parameter	Dimensions (mm)	Parameter	Dimensions (mm)
W_g	17	r_3	1.8
W_S	17	r_4	1.4
L_S	30	S_1	1.6
W_{PG}	4.5	S_2	1.2
L_f	5.73	S_3	1.6
W_f	3	S_4	1.4
L_C	8	E_1	1.6
l_p	12.5	E_2	1.9
w_p	2	E_3	0.9
a	14	E_4	1.1
b	14	E_5	1.6
R	5	E_6	2.9
r_1	2.8	E_7	1.9
r_2	2.3	E_8	1.1

II. PROPOSED ANTENNA DESIGN

Fig. 1 demonstrate the design evolution of the Tri-Quarter Circular (TQC) EWB MIMO antenna with PGP and slotted parasitic strip. The proposed antenna is composed of a three-layered structure in which the top, bottom copper layers are engraved to develop the proposed TQC patch embedded with a microstrip feedline and an altered PGP. The novelty of using a three-fourth circular patch in MIMO systems lies in its unique geometry, which introduces certain characteristics that can be advantageous in specific scenarios. A three-fourth circular (Tri-Quarter Circular) patch refers to a circular patch antenna with approximately 270 degrees of its circumference, leaving one-fourth of the circle open. It can achieve circular polarization or other polarization states, enhancing the system's robustness against signal fading and improving link reliability. It also offer a more compact design compared to a full circular patch while still maintaining some of the circular polarization properties. This design can help in reducing mutual coupling, minimizing interference between antennas, and improving the isolation between MIMO channels.Rogers RT/duroid 5880 substrate with a ϵ_r (dielectric constant) of 2.2 and loss tangent ($\tan\delta$) of 0.0009 placed between the two copper plated layers. A 50 Ω microstrip feedline with a size of L_f and W_f connected at the lower edges of the radiating elements. The overall physical volume of the proposed design is 2.74 λ_0 × 4.83 λ_0 × 0.25 λ_0.

The equivalent circuit of the proposed design is depicted in Fig. 2. The capacitance ($C0$ or $C01$) provided by the EBG structure contributes to the formation of a notch in the

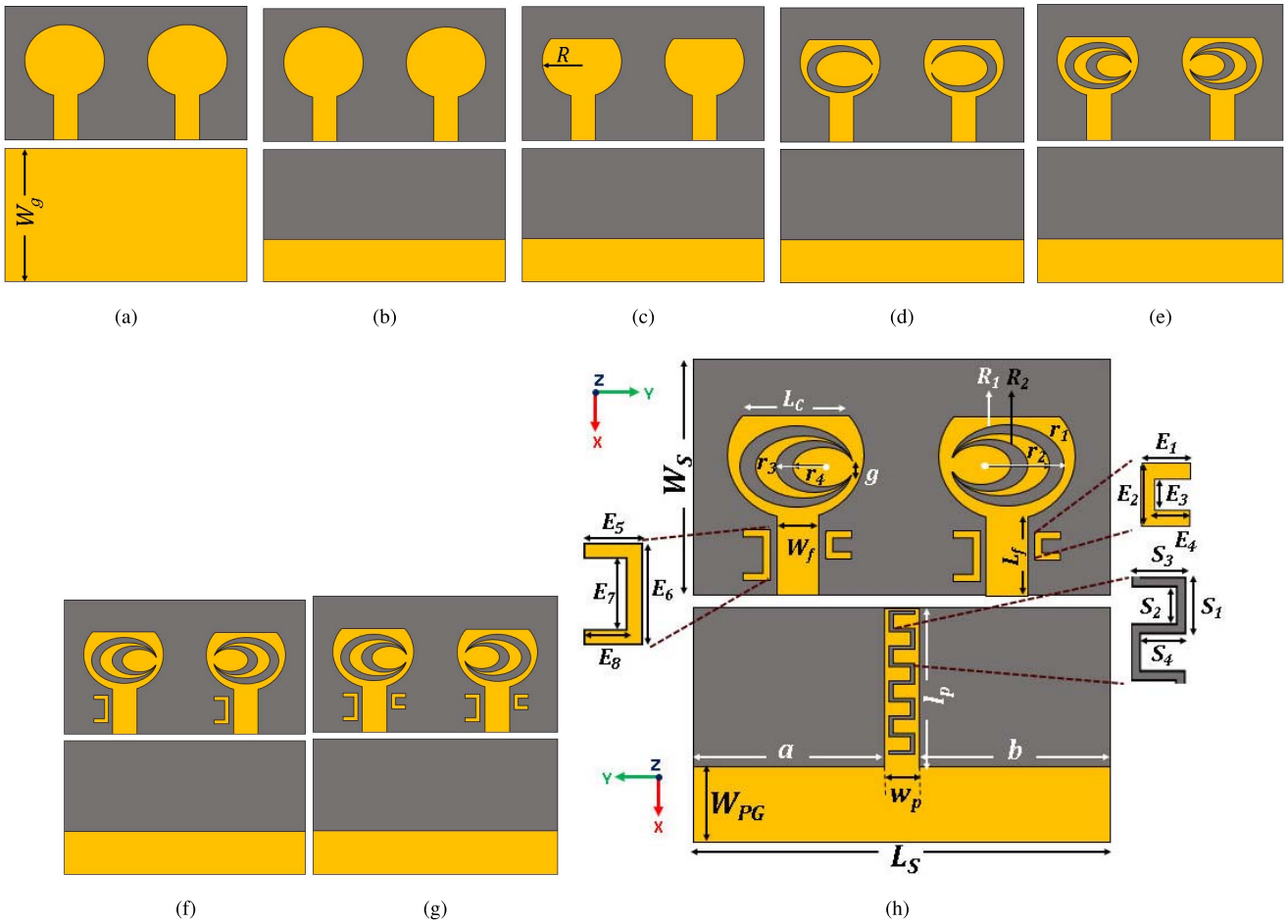

FIGURE 1. Design evolution of proposed TQC EWB MIMO.

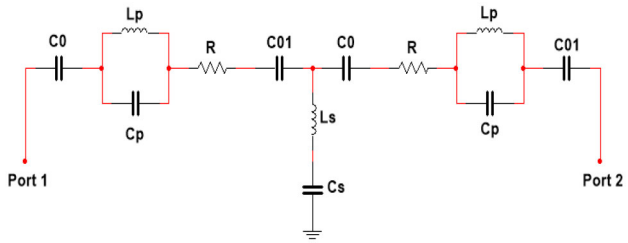

FIGURE 2. Equivalent circuit of the proposed design.

frequency response of the MIMO system. This notch selectively attenuates signals within a specific frequency range, thereby mitigating interference from unwanted frequencies. The L_p, C_p resonance, along with the series resistance 'R', creates a notch in the frequency response of the structure. At the resonant frequency, the impedance of the LC circuit becomes very high, effectively blocking signals in that frequency range. This notch band acts as a filter, attenuating or rejecting signals within a specific frequency range while allowing others to pass through relatively unaffected. When an inductor (L_s) is placed in series with a capacitance (C_s) to form an LC circuit, it can indeed enhance isolation in electromagnetic systems.

By effectively introducing capacitance into the system, the EBG structure alters the electrical characteristics of the environment around the antennas and feedlines, allowing for precise control over the frequency response and interference suppression capabilities of the MIMO system.

III. RESULTS AND DISCUSSION

A. EVOLUTION OF EWB MIMO ANTENNA

The step-by-step design procedure of the basic EWB antenna is given in Fig. 1(a-c) and the reflection coefficients of the respective designs are depicted in Fig. 3. In stage-I, two circular patches having radius 'R', with full ground plane (Fig. 1(a)) attained the bandwidth of 30.5 GHz (12.55 to 43.05 GHz). In stage-II, two patch elements share a rectangular partial ground plane (PGP) of size ($L_s \times W_{PG}$), which is situated beneath the radiating components in order to maintain the antenna's compact design. It results in the enhancement of impedance bandwidth from 30.5 GHz to 64.47 GHz (5.83 to 70.3 GHz). In stage-III, the transformation of circular patch into TQC as shown in Fig. 1(c) achieved the enhanced extremely wideband of 85.8 GHz

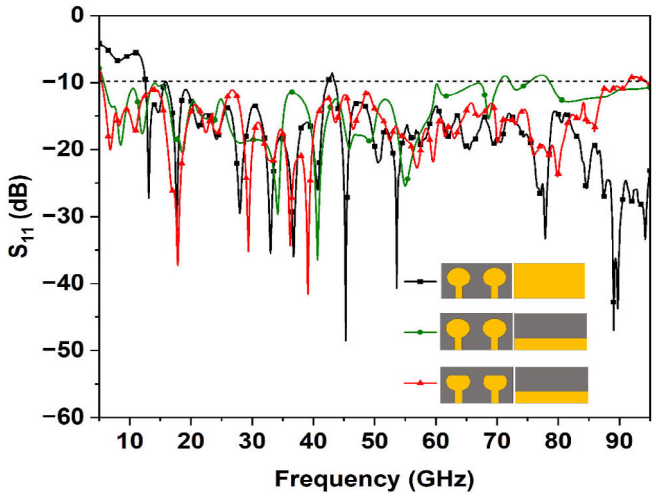

FIGURE 3. S_{11} vs. Frequency plot at different evolution steps of the MIMO antenna.

(5.45 to 91.25 GHz). Further steps in the design evolution to generate the notch-bands are elaborated in Section III-B.

B. ANALYSIS OF BAND-NOTCHED CHARACTERISTICS OF EWB MIMO ANTENNAS

Band-notched UWB antennas are required in order to prevent electromagnetic interference. The fundamental concept underlying the construction of the notch band antenna is that, since the surface current distribution of the radiating element is mostly concentrated on its outside part, the core piece of the antenna element can be deleted without affecting the distribution of current. Two elliptical CO-CSRR namely R_1, R_2 having major and minor radius r_1, r_2, r_3, r_4 respectively are etched on the radiating elements as shown in Figs. 1(f) and 1(g). The wavelength of the resonant elements in the filter, designed to generate a notch band at specific frequencies, can be calculated using the formula (1) [23],

$$\lambda = \frac{c}{f \times \sqrt{\epsilon_{reff}}} \tag{1}$$

$$\sqrt{\epsilon_{reff}} = \frac{\epsilon_r + 1}{2} \tag{2}$$

Equation (1) involves the speed of light denoted by 'c' and the relative permittivity, ϵ_r, which represents the dielectric constant. The radius of the two elliptical CSRR is one-half and 1/4th of the wavelength corresponding to the center frequencies of 10.765 GHz, 14.855 GHz to generate notches at X-band (9.4 to 12.13 GHz) and Ku-band (13.62 to 16.09 GHz). The center frequencies of the first and second notch frequency bands can be determined using the expression (3, 4),

$$f_{cNB1} = \frac{c}{2 \times \left(R_1 \times \sqrt{\epsilon_{reff}}\right)} \tag{3}$$

$$f_{cNB2} = \frac{c}{4 \times \left(R_2 \times \sqrt{\epsilon_{reff}}\right)} \tag{4}$$

where $R_1 = 2R - (r_1 - r_2)$, $R_2 = R - (r_3 + r_4) - g$. When R_1, R_2 engraved on the radiating element, the antenna generates notch bands with center frequencies 10.765 GHz, 14.855 GHz as shown in Fig. 5.

Further analysis is carried out for additional two notches in higher frequency bands. To get third and fourth notch bands, two EBGs are employed on either side of the feedline having one-half and one-fourth wavelengths respectively. The placement of EBGs in a MIMO system involves careful consideration of the system requirements, antenna configurations, and the desired impact on system performance. The advantage of positioning an EBG structure on either side of the feedline in a MIMO system lies in its ability to influence the electromagnetic characteristics of the feedline and enhance overall MIMO performance. Placing EBG structures on either side of the feedline helps improve isolation between adjacent antennas in a MIMO array. The EBG can effectively suppress unwanted coupling and reduce mutual interference, leading to enhanced isolation and improved channel separation. It can aid in controlling the radiation pattern of individual antennas within the MIMO array. This allows for better customization of the antenna radiation characteristics, optimizing the overall system performance in terms of coverage and efficiency.

EBG structures are designed to exhibit band gaps, which are frequency ranges where the propagation of electromagnetic waves is prohibited. When positioned on either side of a feedline, the EBG structure acts as a filter, allowing only certain frequencies to pass through while attenuating or blocking others. By controlling the periodicity and geometry of the EBG elements, engineers can tailor the reflection and transmission properties at specific frequencies. The center frequencies of the third and fourth notch bands can be computed using the (5, 6).

$$f_{cNB3} = \frac{c}{2 \times \left(L_1 \times \sqrt{\epsilon_{reff}}\right)} \tag{5}$$

$$f_{cNB4} = \frac{c}{4 \times \left(L_2 \times \sqrt{\epsilon_{reff}}\right)} \tag{6}$$

where $L_1 = (2E_5 + E_6) - (E_7 + 2E_8)$ and $L_2 = (E_2 + E_3) - 2E_4$. Due to the placement of two EBG structures at the close proximity of the patch, third and fourth notch bands of Q-band downlink (40.6 to 43.07 GHz) and V-band (55.94 to 57.67 GHz) are generated. Figure 4 provides a visualization of the S_{11} characteristics of the individual slots and Electromagnetic Band Gaps (EBGs) responsible for creating the notch bands. Simultaneously, Fig. 5 displays the simulated S_{11} of the entire structure.

The complete structure achieved high return loss of 30.82 dB at 17.58 GHz, 29.10 dB at 24.5GHz, 31.80 dB at 38.12 GHz, 29.50 dB at 44.56 GHz, 30.43 dB at 49.01 GHz and 29.69 dB at 58.91 GHz frequencies.

In the pursuit of performance optimization for MIMO antennas, a comprehensive parametric analysis is conducted, involving the systematic variation of various parameters to attain the desired performance metrics. The geometric configuration and physical design of the radiating elements emerge as crucial factors influencing the overall MIMO

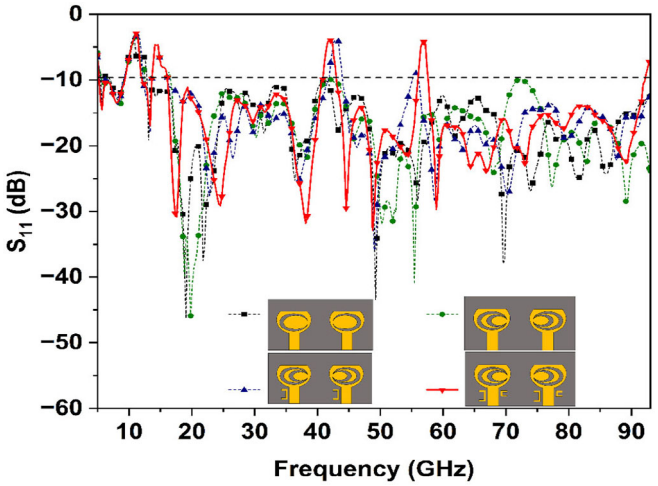

FIGURE 4. Reflection Coefficient for individual slots and EBGs.

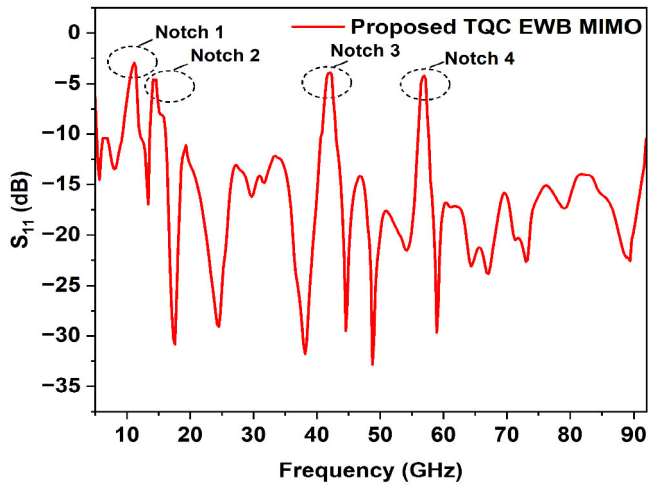

FIGURE 5. Quadruple Notch Band Characteristics of the TQC MIMO.

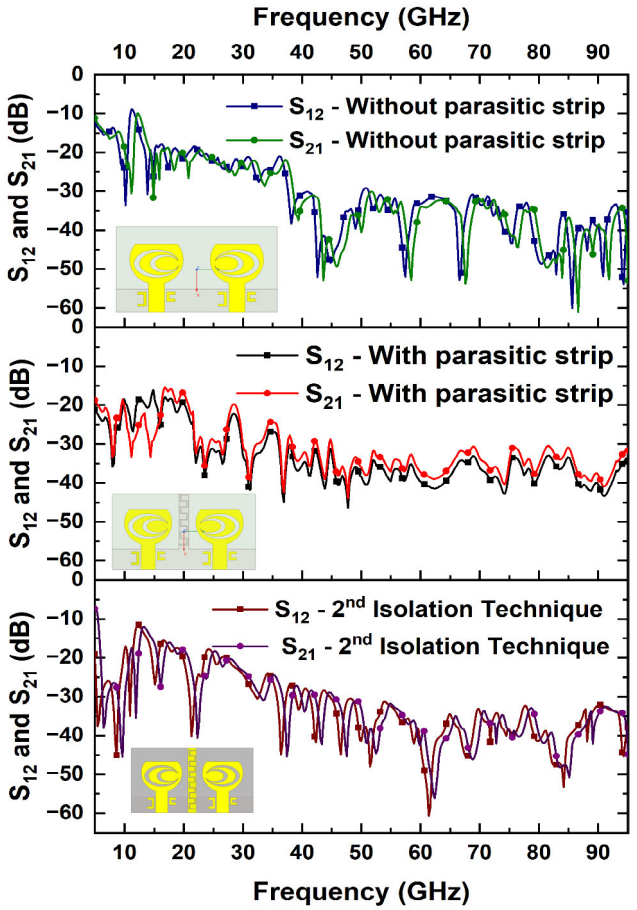

FIGURE 6. S_{12} and S_{21} comparison plot for different isolation techniques.

performance. A parasitic strip is one type of parasitic element that can significantly affect the surface current distribution and, in turn, the overall performance of an antenna in a MIMO system. Usually positioned adjacent to the driven or active antenna elements, a parasitic element is a passive conductor that is not directly linked to the transmitter or receiver. In this design, two isolation techniques are introduced and measured the isolation. In the first technique, the parasitic strip with meandering slot is placed at the rear of the antennas, within the space between them. In the second technique, the meandering slotted parasitic strip is placed in between the radiating elements.

Fig. 7 (a) and (b) illustrates the surface current distribution with and without meander slotted parasitic strip at 5.5 GHz frequency and surface current distribution for the second isolation technique is depicted in 7 (c). Meandering slot acts as a decoupling network and influences the antenna's radiation pattern, reduced the energy directed towards neighbouring antenna, which in turn, enhances the isolation. Meandering slots enable antennas to be packed more densely without sacrificing the performance.

For parametric analysis, simulated results in terms of current distribution, S_{12}, S_{21} parameters are verified and depicted in Fig. 6 and Fig. 7. From the results, it is observed that the isolation is $<$ 10 dB at low frequencies for the proposed design without parasitic strip and second isolation technique. The isolation is in between 17.08 dB to 31.5 dB for the entire EWB range by using the first isolation technique (i.e., the meandering slotted parasitic strip on the GP).

The simulated 2D radiation patterns at specific frequencies, such as 6.5, 17.5, 24.538, 43.3, 66.85 and 70.15 GHz, for both E and H-planes are visually represented in Fig. 8. The radiation characteristics showcase a dipole-like radiation pattern in the XY-plane and a compressed omni-directional pattern in the YZ-plane.

Additional parametric analysis has been conducted to investigate the gap variation between the Patch and EBG structures, denoted by the variable 'D'. The reflection coefficient has been meticulously examined by varying the values of 'D', and the simulation results have been visually represented in Fig. 9. It is noteworthy that the proposed antenna demonstrates optimal notch bands when 'D' is set to 1.73 mm.

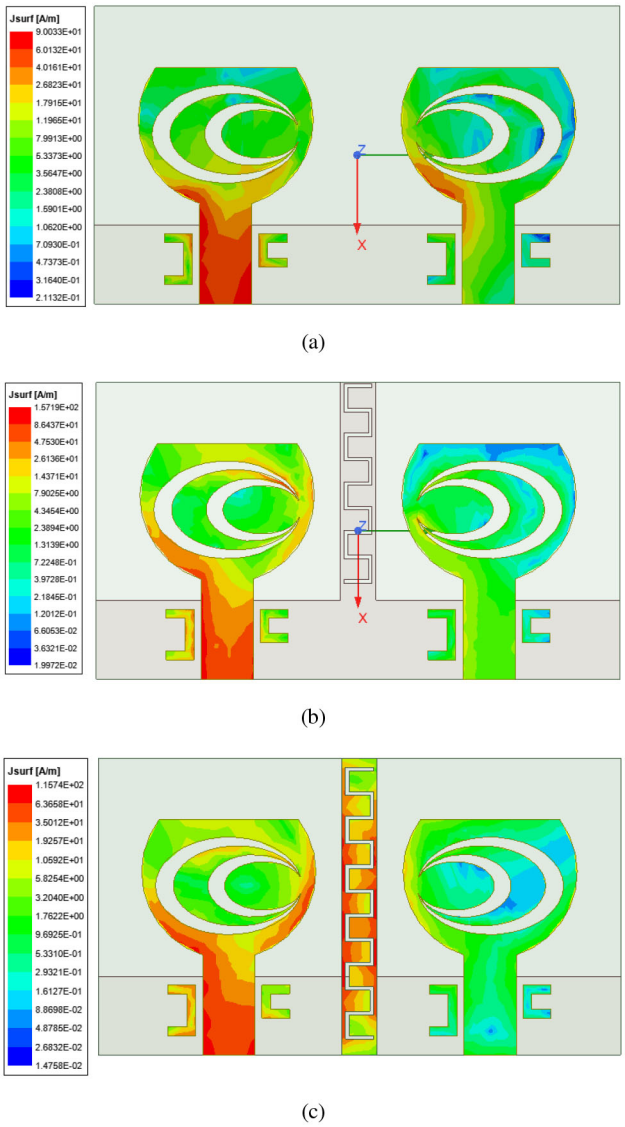

FIGURE 7. Surface current distribution (a) with slotted parasitic strip on GP (b) without slotted parasitic strip on GP (c) with slotted parasitic strip in between the radiating elements.

The gain in a MIMO system signifies the measure of the antenna's ability to direct or concentrate the transmitted or received signal in a specific direction compared to a reference antenna. Fig. 10 illustrates the simulated gain for the proposed TQC MIMO. Notably, the gain ranges from 3.32 to 8.9 dBi within the EWB frequency range.

C. TWO PORT MIMO ANTENNA DIVERSITY PARAMETER ANALYSIS

The diversity parameters in MIMO systems are vital for improving the reliability, performance, and robustness of wireless communication. They enable MIMO systems to make efficient use of multiple antennas to mitigate the challenges posed by fading, interference, and variable channel conditions, ultimately delivering high-quality and high-capacity wireless services.

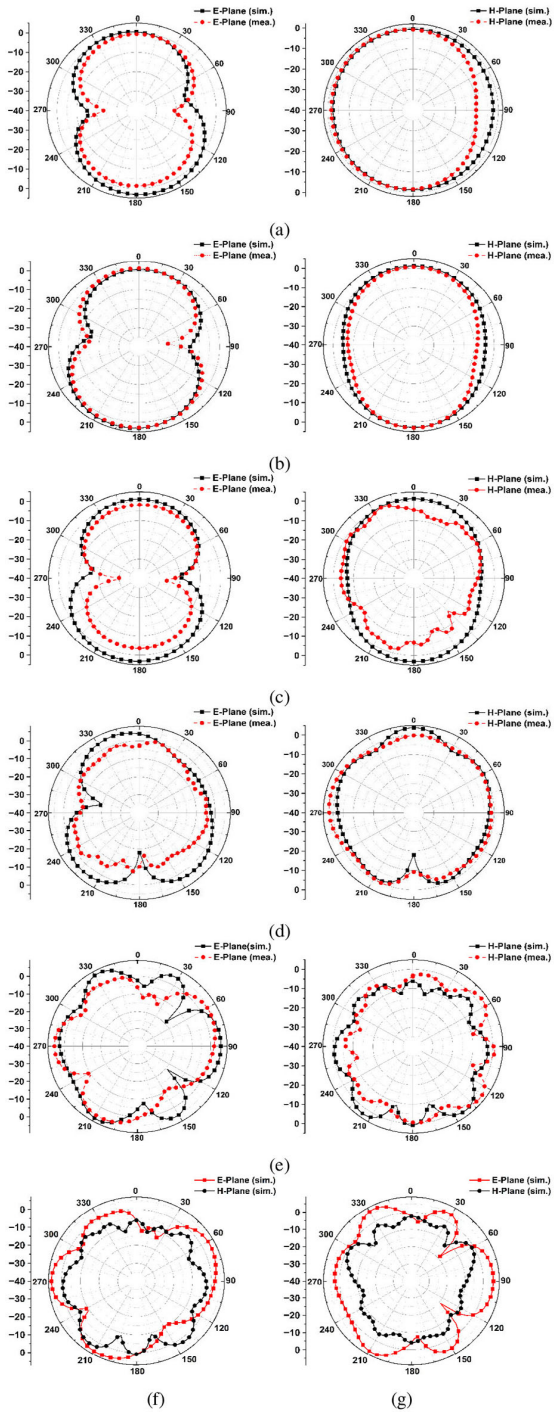

FIGURE 8. 2d Radiation pattern of the proposed antenna (a) 6.5 GHz (b) 17.5 GHz (c) 24.5 GHz (d) 38GHz (e) 43.3 GHz (f) 66.85 GHz (sim.) (g) 70.15 GHz (sim.).

1) ENVELOPE CORRELATION COEFFICIENT (ECC)

The ECC quantifies the correlation between the envelopes of two received signals from different antennas. In the context of spatial diversity, lower ECC values indicate reduced correlation between signals received by different antennas.

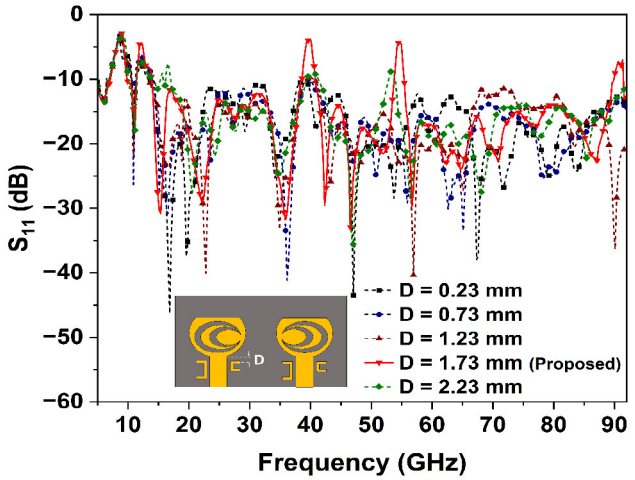

FIGURE 9. S_{11} for different 'D' values.

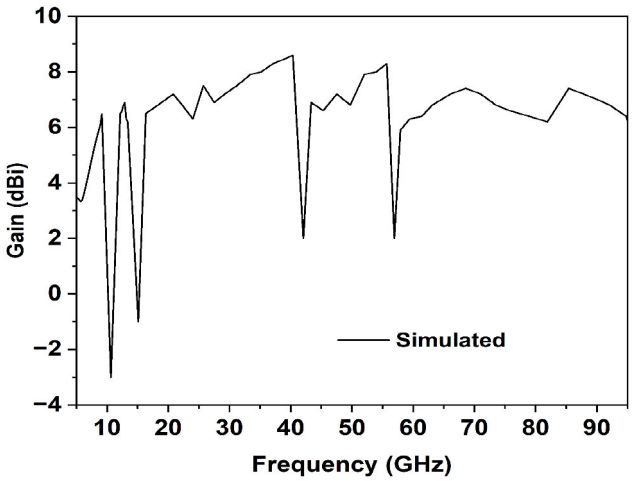

FIGURE 10. Gain vs. Frequency (GHz) for the entire achieved EWB.

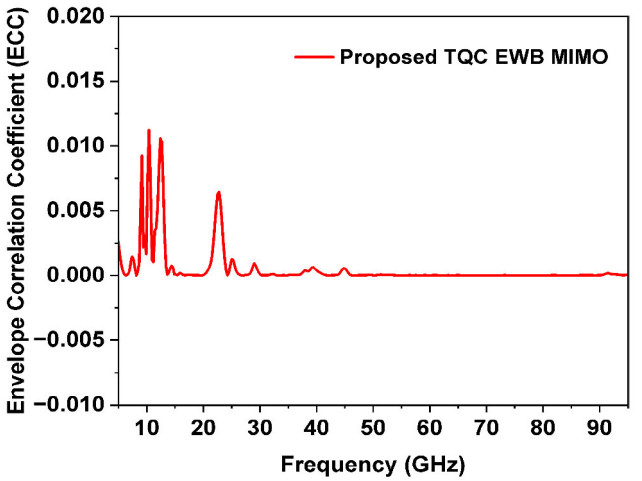

FIGURE 11. Envelope Correlation Coefficient vs. Frequency.

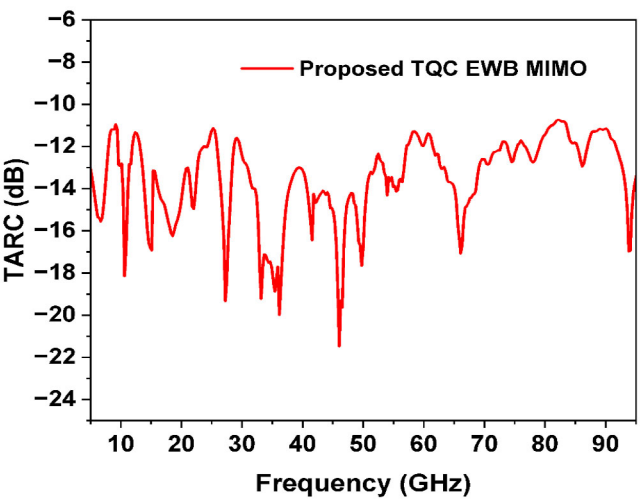

FIGURE 12. TARC vs. Frequency (GHz).

Evaluating ECC is crucial in MIMO system design and implementation to maximize wireless communication quality and reliability. In pursuit of enhanced communication, an optimal ECC value is typically less than 0.5. The ECC of the proposed MIMO design can be computed using (7), [24],

$$ECC = \frac{\left|\int\int_{4\pi}\left[E_i(\theta,\phi)\times E_j(\theta,\phi)\right]d\Omega\right|^2}{\int\int_{4\pi}|E_i(\theta,\phi)|^2 d\Omega \times \int\int_{4\pi}\left|E_j(\theta,\phi)\right|^2 d\Omega} \quad (7)$$

The ECC value is plotted in Fig. 11, and it is within an acceptable range. A maximum value of 0.011 was noted.

2) TOTAL ACTIVE REFLECTION COEFFICIENT (TARC)

TARC is an essential attribute in the MIMO structure that is used in the design and assessment of wireless communication systems. It includes active elements such as matching networks and measures the reflection coefficient perceived by the transmitter at the antenna system's input. A higher TARC value implies a reduction in performance, as it indicates that a portion of the incident power is being reflected back to the transmitter. Therefore, while designing a MIMO antenna, minimising TARC becomes essential. Equation (8) [12] is used to compute the TARC.

$$TARC = \sqrt{\frac{\left|\left(S_{11}+S_{12}e^{j\theta}\right)\right|^2 + \left|\left(S_{21}+S_{22}e^{j\theta}\right)\right|^2}{2}} \quad (8)$$

The TARC response of the proposed design is illustrated in Fig. 12. The TARC value, registering at less than −10 dB, signifies a commendable level of isolation between the radiating elements.

3) DIVERSITY GAIN (DG)

Diversity gain is another crucial factor, which is determined by (9) and represents the improvement in system performance as a result of the diversity technique. The performance of the system improves with increasing diversity gain value. Its value should be around to 10 for MIMO antenna performance that meets requirements. The achieved

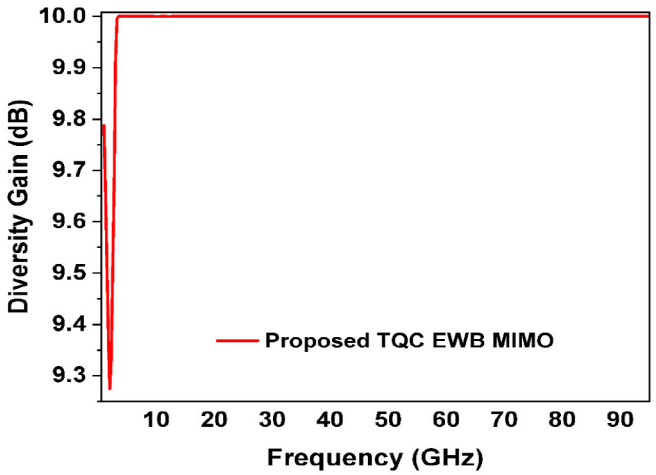

FIGURE 13. Diversity Gain vs. Frequency (GHz).

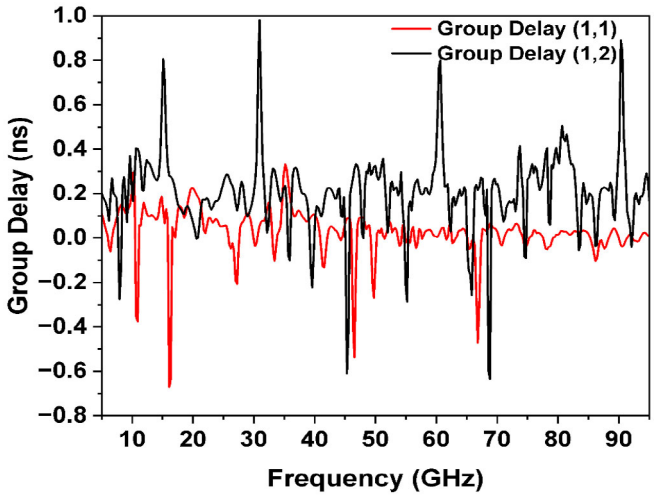

FIGURE 14. Group delay (ns).

DG value is ≅ 10, depicted in Fig. 13 and it was calculated using (9) [25], ECC based on scattering parameters.

$$DG = 10\sqrt{1 - (ECC)^2} \tag{9}$$

4) GROUP DELAY (GD)

Group Delay is one of the significant performance parameters for EWB antenna. An unexpectedly distorted signal will be detected if the group delay is different for each frequency that the antenna supports. Fig. 14 describes that there is very little group delay for the entire EWB, which is approximately the same. It fluctuates between 0.2 ns to −0.25 ns, with the exception of four particular frequencies.

Fig. 15 (a) represents the fabricated prototype top-view, bottom-view and the measurement setup is depicted in Fig. 15 (b). Due to the VNA's availability limited to 43.5 GHz, the measurements were conducted up to the maximum frequency offered by the equipment. The simulated and the measured results portrayed in

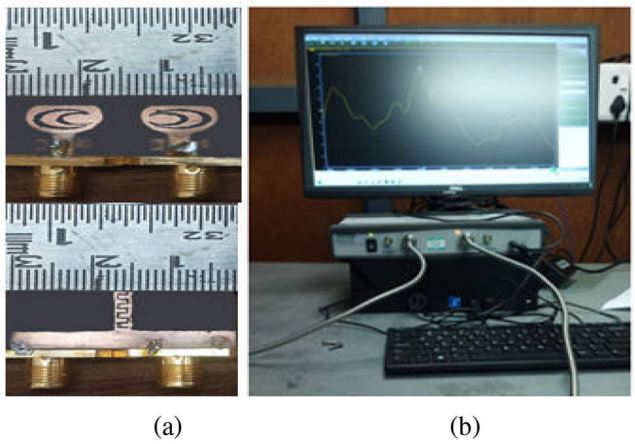

FIGURE 15. Fabricated Prototype and Measurement setup.

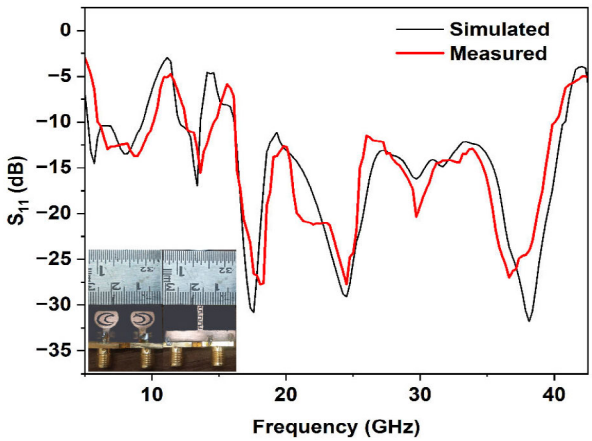

FIGURE 16. S_{11} vs. Frequency - Simulated vs. Measured - upto 43.5 GHz.

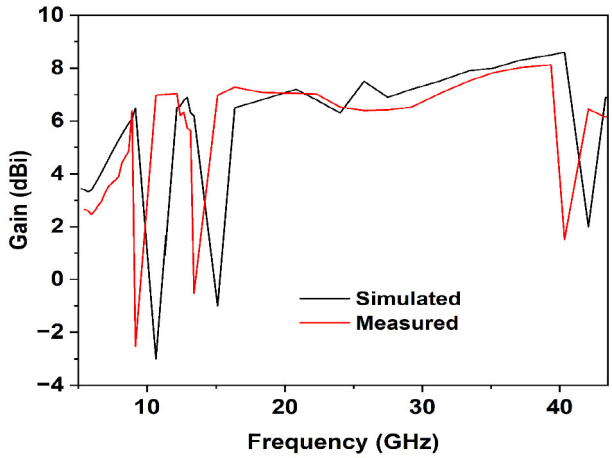

FIGURE 17. Gain (dBi) vs. Frequency - upto 43.5 GHz.

Figs. 16 and 17 are in good agreement and slight variations are observed in the measured results due to the fabrication losses.

The comparative analysis of the proposed antenna in terms of isolation, gain, ECC, TARC and diversity gain is

TABLE 2. Parametric comparison of the TQC MIMO with conventional antennas.

Ref. No.	Dimension	Bandwidth (GHz)	Frequency range (GHz)	No. of elements	No. of notch bands	Isolation (dB)	Gain (dBi)	ECC	TARC	DG (dB)
[3]	2.12 λ_0 x 2.12 λ_0	21.5	2.5 to 24	8	-	$>$ 23	8	-	-	-
[4]	0.68 λ_0 x 1.37 λ_0	17.1	2.9 to 20	2	1	$>$20	1.6 to 6	$<$0.012	-	$>$9.7
[8]	0.03 λ_0 x 0.22 λ_0	0.4, 0.775	3.4 to 3.8, 5.15 to 5.925	10	-	$>$20	5.9	$<$0.06	-	-
[9]	1.85 λ_0 x 0.98 λ_0	0.9	3.1 to 4.1	18	-	$>$20	5.3	$<$0.01	-	-
[12]	2.15 λ_0 x 4.46 λ_0	55.9	4.1 to $>$ 60	2	1	$>$15	9	$\leq$0.01	$<$ - 10	$\cong$ 10
[13]	1.39 λ_0 x 0.97 λ_0	9	2 to 11	2	3	$>$15	5	$\leq$0.02	-	-
[16]	3.80 λ_0 x 3.50 λ_0	38.5	1.5 to 40	2	1	$>$20	7.6	$<$0.005	$<$-15	9.99
[17]	0.25 λ_0 x 0.50 λ_0	36.25	4 to 40.25	2	3	$>$ 24	2.2 to 8.6	$<$0.01	$<$- 10	-
[21]	4.14 λ_0 x 4.14 λ_0	37.1	2.9 to 40	4	-	$>$17	4.3 to 13.5	$<$0.04	$<$- 10	9.5
[26]	0.82 λ_0 x 0.82 λ_0	9.5	2.5 to 12	4	3	$>$15	2.5 to 5.5	$<$0.05	$<$ 0	-
[27]	0.50 λ_0 x 0.82 λ_0	7.5	3.1 to 10.6	2	1	$>$15	1 to 5	-	-	-
[28]	0.63 λ_0 x 0.63 λ_0	8.7	2.9 to 11.6	2	2	$>$16	7	$<$0.02	-	-
[29]	1.04 λ_0 x 1.04 λ_0	11.45	2.30 to 13.75	4	3	$>$22	1.40 to 4.60	$<$0.02	$<$ -10	9.5
[30]	0.63 λ_0 x 0.85 λ_0	10.9	3.1 to 14	2	1	$>$23	1.1 to 5.8	$<$0.002	-	$>$ 9.98
[31]	1.34 λ_0 x 1.34 λ_0	8.7	3.1 to 11.8	4	3	$>$20	6.35	$<$0.001	-	$>$ 9.99
Proposed work	2.74 λ_0 $\times$ 4.83 λ_0	85.8	5.45 to 91.25	2	4	$>$31.5	8.9	$<$0.011	$<$-10	$\cong$ 10

performed and tabulated in Table 2. Through the conducted analysis, it has been observed that the proposed antenna exhibits a significantly reduced size while achieving an exceptionally wideband coverage, accompanied by suitable gain and high isolation of 31.5 dB. Importantly, these achievements are realized without compromising the overall performance of the antenna. The proposed antenna design offers notable advantages, including high isolation, multiple notch characteristics, extremely wideband capability, and compact size. These features collectively enhance its suitability for various applications like Radar systems, 5G and beyond, Satellite communication, Millimeter wave communication, wireless sensor networks, medical imaging. While the simulated performance is promising, real-world implementation may face challenges such as manufacturing tolerances, material properties, and environmental factors that could affect performance.

IV. CONCLUSION

In this research article, a novel and miniaturized CO-CSRR loaded TQC extremely wideband MIMO is designed, simulated and fabricated. The proposed structure achieved the EWB of 85.8 GHz (5.45 to 91.25 GHz) with quadruple notch bands X-band (9.4 to 12.13 GHz) and Ku-band (13.62 to 16.09 GHz), Q-band downlink (40.6 to 43.07 GHz) and V-band (55.94 to 57.67 GHz) respectively. Two different isolation techniques are introduced and comparative analysis is performed in terms surface current distribution and S_{12} and S_{21}. The isolation parameter has been validated for two distinct positions of the meandering slotted parasitic strip. The proposed antenna with the meandering slotted parasitic strip placed on the GP achieved the high isolation of 31.5 dB. The compactness of the antenna is highly increased without effecting the performance. It achieved the high return loss of 30.82 dB at 17.58 GHz, gain of 8.9 dBi, ECC $<$ 0.011, TARC $<$ $-$10 dB, Group Delay $<$ 0.2 ns, Diversity gain $\cong$ 10 dB. The parametric comparison with conventional MIMO antennas is performed and tabulated in Table 2.

ACKNOWLEDGMENT

The authors express their sincere gratitude to the management of VIT-AP University and the SENSE department for their unwavering support and encouragement throughout the course of this endeavor.

REFERENCES

[1] S. Koziel and A. Bekasiewicz, "Electromagnetic-simulation-driven design of compact ultra-wideband multiple-input multiple-output antenna," *Microw., Antennas Propag.*, vol. 10, no. 15, pp. 1721–1724, 2016.

[2] B. T. Ahmed and I. F. Rodríguez, "Compact high isolation UWB MIMO antennas," *Wireless Netw.*, vol. 28, pp. 1977–1999, Jul. 2022. [Online]. Available: https://doi.org/10.1007/s11276-022-02951-9

[3] A. Mohanty and S. Sahu, "Design of 8-port compact hybrid fractal UWB MIMO antenna with a conjoined reflector-ground integration for isolation improvement," *AEU Int. J. Electron. Commun.*, vol. 145, Feb. 2022, Art. no. 154102.

[4] R. Chandel and A. K. Gautam, "Compact MIMO/diversity slot antenna for UWB applications with band-notched characteristic," *Electron. Lett.*, vol. 52, no. 5, pp. 336–338, 2016.

[5] H. S. Mewara, J. K. Deegwal, and M. M. Sharma, "A slot resonators based quintuple band-notched Y-shaped planar monopole ultra-wideband antenna," *AEU-Int. J. Electron. Commun.*, vol. 83, pp. 470–478, Jan. 2018.

[6] X. Cao, Y. Xia, L. Wu, L. Lang, and L. Cui, "The design of a compact quintuple band-notched UWB antenna," *Progr. Electromagn. Res.*, vol. 97, pp. 241–253, Dec. 2019.

[7] D. Srikar et al., "A novel integrated UWB sensing and 8-element MIMO communication cognitive radio antenna system," *Electron*, vol. 12, no. 2, p. 330, 2023. [Online]. Available: https://doi.org/10.3390/electronics12020330

[8] N. Jaglan, S. D. Gupta, B. K. Kanaujia, and M. S. Sharawi, "10 element sub-6-GHz multi-band double-T based MIMO antenna system for 5G smartphones," *IEEE Access*, vol. 9, pp. 118662–118672, 2021.

[9] N. Jaglan, S. D. Gupta, and M. S. Sharawi, "18 element massive MIMO/diversity 5G smartphones antenna design for sub-6 GHz LTE bands 42/43 applications," *IEEE Open J. Antennas Propag.*, vol. 2, pp. 533–545, 2021.
[10] D. Lodhi and S. Singhal, "CPW fed shovel shaped super wideband MIMO antenna for 5G applications," *AEU-Int. J. Electron. Commun.*, vol. 168, Aug. 2023, Art. no. 154700.
[11] M. Sood and A. Rai, "Wideband 4-port MIMO antenna array using fractal and complimentary split-ring structure for Ku-band appliances," *AEU-Int. J. Electron. Commun.*, vol. 172, Dec. 2023, Art. no. 154970.
[12] A. Baz, D. Jansari, S. P. Lavadiya, and S. K. Patel, "Miniaturized and high gain circularly slotted 4×4 MIMO antenna with diversity performance analysis for 5G/Wi-Fi/WLAN wireless communication applications," *Results Eng.*, vol. 20, Dec. 2023, Art. no. 101505.
[13] N. Jaglan, S. D. Gupta, E. Thakur, D. Kumar, B. K. Kanaujia, and S. Srivastava, "Triple band notched mushroom and uniplanar EBG structures based UWB MIMO/Diversity antenna with enhanced wide band isolation," *AEU Int. J. Electron. Commun.*, vol. 90, pp. 36–44, Jun. 2018.
[14] I. Ud Din et al., "High performance antenna system in MIMO configuration for 5G wireless communications over sub-6 GHz spectrum," *Radio Sci.*, vol. 58, no. 10, pp. 1–22, 2023.
[15] R. K. Mistri et al, "Quad element MIMO antenna for C, X, Ku, and Ka-band applications," *Sensors*, vol. 23, no. 20, p. 8563, 2023.
[16] G. Saxena, P. Jain, and Y. K. Awasthi, "High diversity gain super-wideband single band-notch MIMO antenna for multiple wireless applications," *IET Microw. Antennas Propag.*, vol. 14, no. 1, pp. 109–119, 2020.
[17] T. Hemalatha and B. Roy, "Ground plane alteration extremely wideband SPAS pair-based MIMO antenna with improved isolation and band notched characteristics," *AEU Int. J. Electron. Commun.*, vol. 176, Mar. 2024, Art. no. 155118.
[18] R. Cicchetti, E. Miozzi, and O. Testa, "Wideband and UWB antennas for wireless applications: A comprehensive review," *Int. J. Antennas Propag.*, vol. 2017, Feb. 2017, Art. no. 2390808.
[19] D. Q. Liu, H. J. Luo, M. Zhang, H. L. Wen, B. Wang, and J. Wang, "An extremely low-profile wideband MIMO antenna for 5G smartphones," *IEEE Trans. Antennas Propag.*, vol. 67, no. 9, pp. 5772–5780, Sep. 2019.
[20] M. A. Ul Haq and S. Koziel, "Feedline alterations for optimization-based design of compact super-wideband MIMO antennas in parallel configuration," *IEEE Antennas Wireless Propag. Lett.*, vol. 18, no. 10, pp. 1986–1990, Oct. 2019.
[21] C. Yu et al., "A super-wideband and high isolation MIMO antenna system using a windmill-shaped decoupling structure," *IEEE Access*, vol. 8, pp. 115767–115777, 2020.
[22] S. Dey, M. S. Arefin, and N. C. Karmakar, "Design and experimental analysis of a novel compact and flexible super wide band antenna for 5G," *IEEE Access*, vol. 9, pp. 46698–46708, 2021.
[23] R. B. Keller,. "Frequency and wavelength," in *Design for Electromagnetic Compatibility: In a Nutshell*. Cham, Switzeralnd: Springer, 2023. [Online]. Available: https://doi.org/10.1007/978-3-031-14186-74
[24] Z. Zhou, Y. Ge, J. Yuan, Z. Xu, and Z. D. Chen, "Wideband MIMO antennas with enhanced isolation using coupled CPW transmission lines," *IEEE Trans. Antennas Propag.*, vol. 71, no. 2, pp. 1414–1423, Feb. 2023, doi: 10.1109/TAP.2022.3232693.
[25] H.-H. Tran, T. The-Lam Nguyen, and T. N. Thi, "Two closely spaced microstrip patches with high isolation for full-duplex/MIMO applications," *PLoS One*, vol. 18, no. 10, 2023, Art. no. e0290980.
[26] Z. Chen, W. Zhou, and J. Hong, "A miniaturized MIMO antenna with triple band-notched characteristics for UWB applications," *IEEE Access*, vol. 9, pp. 63646–63655, 2021.
[27] L. Liu, S. W. Cheung, and T. I. Yuk, "Compact MIMO antenna for portable UWB applications with band-notched characteristic," *IEEE Trans. Antennas Propag.*, vol. 63, no. 5, pp. 1917–1924, May 2015, doi: 10.1109/TAP.2015.2406892.
[28] Z. Li, C. Yin, and X. Zhu, "Compact UWB MIMO Vivaldi antenna with dual band-notched characteristics," *IEEE Access*, vol. 7, pp. 38696–38701, 2019, doi: 10.1109/ACCESS.2019.2906338.
[29] Z. Tang, X. Wu, J. Zhan, S. Hu, Z. Xi, and Y. Liu, "Compact UWB-MIMO antenna with high isolation and triple band-notched characteristics," *IEEE Access*, vol. 7, pp. 19856–19865, 2019.
[30] M. Awais, S. Bashir, A. Khan, M. Asif, N. Ullah, and H. I. Alkhammash, "A novel compact highly isolated UWB MIMO antenna with WLAN notch," *Comput. Mater. Continua*, vol. 75, no. 1, pp. 669–681, 2023.
[31] A. Abbas et al., "Highly selective multiple-notched UWB-MIMO antenna with low correlation using an innovative parasitic decoupling structure," *Int. J. Eng. Sci. Technol.*, vol. 43, Jul. 2023, Art. no. 101440.

HEMALATHA T (Member, IEEE) received the B.Tech. degree in electronics and communication from the Vijaya Institute of Technology for Women, Vijayawada, in 2013 and the M.Tech. degree in embedded systems from the Lingayas Institute of Technology in 2015. She is currently pursuing the Ph.D. degree in electronics and communication engineering with VIT-AP University, Amaravati. Her research interests includes reduced-complexity MIMO design and UWB MIMO notch band characteristics.

BAPPADITTYA ROY (Senior Member, IEEE) received the B.Tech. and M.Tech. degrees in electronics and communication engineering in 2008 and 2011, respectively, and the Ph.D. degree in electronics and communication from the National Institute of Technology at Durgapur, Durgapur, in 2018. He is the author of a few books, more than 50 articles. His research interests include high-frequency and wearable antenna design and substrate characteristic processes and applications. He received a research grant and different research awards for excellence.